OXFORD JLB JOURNAL OF LEUKOCYTE BIOLOGY

Journal of Leukocyte Biology, 2023, **113**, 71–83

https://doi.org/10.1093/jleuko/qiac008

Regular Article

Galectin-4 increases the ability of M2 macrophages to enhance antiviral CD4$^+$ T-cell responses

In-Gu Lee,[1] Yong-Hyun Joo,[1] Hoyeon Jeon,[1] Raehyuk Jeong,[1] Eui Ho Kim,[2] Hyunwoo Chung,[3] Seong-il Eyun,[1] Jeongkyu Kim,[1,*] Young-Jin Seo,[1,*,†] and So-Hee Hong[4,*]

[1]Department of Life Science, Chung-Ang University, 84 Heukseok-ro, Dongjak-gu, Seoul 06974, Republic of Korea
[2]Viral Immunology Laboratory, Institut Pasteur Korea, 16 Daewangpangyo-ro 712 beon-gil, Bundang-gu, Seongnam 13488, Republic of Korea
[3]Laboratory of Immune System Biology, National Institute of Allergy and Infectious Diseases, National Institutes of Health, 9000 Rockville Pike, Bethesda, MD 20892, USA
[4]Department of Microbiology, College of Medicine, Ewha Womans University, 25 Magokdong-ro 2-gil, Gangseo-gu, Seoul 07804, Republic of Korea
Corresponding authors: Young-Jin Seo, Department of Life Science, Chung-Ang University, 84 Heukseok-ro, Dongjak-gu, Seoul 06974, Republic of Korea. Email: yjseo@cau.ac.kr; So-Hee Hong, Department of Microbiology, College of Medicine, Ewha Womans University, 25 Magokdong-ro 2-gil, Gangseo-gu, Seoul 07804, Republic of Korea. Email: hongsohee@gmail.com; Jeongkyu Kim, Department of Life Science, Chung-Ang University, 84 Heukseok-ro, Dongjak-gu, Seoul 06974, Republic of Korea. Email: kimj@cau.ac.kr

Abstract

Galectin-4 (Gal-4) is a β-galactoside–binding protein belonging to the galectin family. Although Gal-4 is known to be involved in several physiologic processes of the gastrointestinal tract, its immunomodulatory roles remain unclear. In this study, we investigated whether Gal-4 influences the function of M1 and M2 macrophages. Gal-4 treatment drove more robust changes in the gene expression of M2 macrophages compared to M1 macrophages. Antiviral immune response–related genes were significantly upregulated in Gal-4–treated M2 macrophages. Gal-4 significantly enhanced the immunostimulatory activity of M2 macrophages upon Toll-like receptor 7 stimulation or infection with lymphocytic choriomeningitis virus (LCMV). Moreover, the antibody production against LCMV infection and the antiviral CD4$^+$ T-cell responses, but not the antiviral CD8$^+$ T-cell responses, were greatly increased by Gal-4–treated M2 macrophages in vivo. The present results indicate that Gal-4 enhances the ability of M2 macrophages to promote antiviral CD4$^+$ T-cell responses. Thus, Gal-4 could be used to boost antiviral immune responses.

Keywords: galectin-4, M1 macrophage, M2 macrophage, CD4$^+$ T cell, lymphocytic choriomeningitis virus

Abbreviations: BSA, bovine serum albumin; CRD, carbohydrate recognition domain; DEGs, differentially expressed genes; ELISA, enzyme-linked immunosorbent assay; Gal-4, galectin-4; GC, geminal center; GO, gene ontology; GP, glycoprotein; GSEA, gene set enrichment analysis; KEGG, Kyoto Encyclopedia of Genes and Genome; LCMV, lymphocytic choriomeningitis virus; LPS, lipopolysaccharide; NP, nucleoprotein; PBS, phosphate-buffered saline; RBCs, red blood cells; RNA-seq, RNA sequencing; SAM, sequence alignment map; TAMs, tumor-associated macrophages; T_{fh}, follicular helper T; TLR7, Toll-like receptor 7.

1 Introduction

Macrophages are myeloid lineage immune cells circulating in the bloodstream or residing in the tissues and play critical roles in innate immune responses, including the maintenance of tissue homeostasis and the promotion of inflammation processes.[1–4] Macrophages have diverse origins and exhibit distinct phenotypes and functional features depending on their microenvironment. In the early 1990s, the terms *M1* and *M2* were introduced when differential effects of in vitro stimulation with IFN-γ/lipopolysaccharide (LPS) in comparison to IL-4 on macrophage gene expression were described.[5,6] Macrophage nomenclature has since diversified to reflect the continuum between M1-like and M2-like phenotypes. For example, the M2 response has been further classified (M2a, M2b, etc.) depending on the differentiation-inducing agent and the molecular markers expressed. To avoid this complexity, Murray et al.[7] proposed a nomenclature linked to the activation standards, such as M(IL-4), M(IFN-γ), and M(LPS). These stereotyped responses seem to be only fully recognized in vitro, but M1-like and M2-like phenotypes are readily identified in physiologic contexts. In immune responses to pathogens, including viruses, M1 macrophages elicit the initial inflammatory responses to stimulate other immune cells at the early stages of infection, leading to the elimination of pathogens. However, uncontrolled M1 responses cause systemic inflammatory responses, ultimately leading to tissue damage and multiple organ failure in the acute phase of pathogen infection or autoimmune disease.[8–10] By contrast, M2 macrophages are responsible for resolving the inflammatory responses and healing damaged tissues at the late stages of infection, indicating their immunosuppressive properties.[11–13] In addition, biased differentiation or reprogramming into M2 macrophages assists the persistence of chronic viruses and the progression of tumors.[4,14,15] Thus, an improved molecular and spatial understanding of orchestrated involvements of M1 and M2 macrophages in the immune responses to pathogens and the underlying mechanisms of how their activation is modulated will undoubtedly

† Lead author.

Received: July 19, 2022. **Editorial Decision:** November 3, 2022

aid in the determination of specific treatments for infectious diseases.

Galectins are a family of soluble proteins that share a conserved carbohydrate recognition domain (CRD) with a high affinity for β-galactoside residues. They regulate immune responses and have been proposed to be involved in diverse cellular processes, including cell proliferation, differentiation, activation, and apoptosis.[16–19] It is perhaps not surprising that galectins are emerging targets in cellular pathophysiologic processes. Gene expression profiles of galectins show large variations across developmental stages and fluctuate in immune responses to infection.[20–22] To date, 15 galectins have been discovered in mammals, among which 12 have been identified in humans.[20,23,24] Of these, galectin-4 (Gal-4), a tandem-repeat type of galectin with 2 CRD domains, is highly expressed in the epithelial cells of the gastrointestinal tract.[25–28] Intriguingly, however, its role in mucosal immune regulation remains controversial. While Hokama et al.[29] showed that Gal-4 induces the production of IL-6 from $CD4^+$ T cells, exacerbating intestinal inflammation, Paclik et al.[30] reported that Gal-4 reduces intestinal inflammation by inducing selective apoptosis of peripheral and mucosal T cells. Interestingly, Gal-4 is endogenously expressed in IL-4–stimulated M2 macrophages[31] and is proposed to regulate the function and differentiation of monocytes.[32] These studies suggest an involvement of Gal-4 in immune responses dependent on macrophage activation status.

Given the important role of macrophages in host immune responses upon viral infection, we investigated the effect of Gal-4 on M1 and M2 macrophages. We identified a novel role for Gal-4 in the antiviral immune responses of M2 macrophages, which has important implications for viral infection-induced inflammations and, more broadly, for the maintenance of tissue homeostasis.

2 Materials and Methods

2.1 Mice

Male C57BL/6 mice (6–8 weeks old) were purchased from Dae-Han Bio-Link (Eumseong-Gun, Chungcheongbuk-do, Republic of Korea) and housed in the pathogen-free animal facility at the Institut Pasteur Korea. Animal care and experiments were handled in accordance with the animal protocols approved by the Institutional Animal Care and Use Committee at Institut Pasteur Korea (approval number: IPK-21002).

2.2 Cell culture

Cells were cultured with RPMI-1640 or Dulbecco's modified Eagle's medium (GenDepot, Katy, TX, USA) containing 10% fetal bovine serum (GenDepot) and 1% penicillin/streptomycin (Welgene, Seoul, Korea) at 37°C, 5% CO_2.

2.3 Macrophages

Murine macrophages were differentiated from bone marrow cells, as described previously.[33] Briefly, mouse femurs and tibias were flushed with phosphate-buffered saline (PBS) and filtered through a 70-μm cell strainer, and then the red blood cells (RBCs) were removed with RBC lysis buffer (Thermo Fisher Scientific, Waltham, MA, USA). Bone marrow cells were cultured in RPMI-1640 supplemented with macrophage-colony stimulating factor (PeproTech, Cranbury, NJ, USA) for 6 d to obtain the resting (M0) macrophages. M1 and M2 macrophages were polarized by treatment with 100 ng/mL LPS (Sigma-Aldrich, Burlington, MA, USA) for 24 h and 10 ng/mL IL-4 (BioLegend, San Diego, CA, USA) for 48 h, respectively. Successful polarization of M1 and M2 macrophages was verified by measuring the transcription levels of *iNOS* (M1 polarization marker) and *Arg1/Ym1* (M2 polarization markers) (Supplementary Fig. 1). Murine Gal-4 was purchased from R&D Systems (Minneapolis, MN, USA), and 10 μg/mL Gal-4 was applied to M1 or M2 macrophages. Anti–Gal-4 antibody (GeneTex, Irvine, CA, USA) and anti-mouse CD14 antibody (BioLegend) were used for blocking experiments.

2.4 Virus and infection

Lymphocytic choriomeningitis virus (LCMV; Armstrong strain) was propagated in baby hamster kidney cells. Virus titrations were determined by the focus-forming assay, as described previously.[34] For in vitro infection, macrophages were infected with a multiplicity of infection value of 3 or 10.

2.5 Enzyme-linked immunosorbent assay

To detect TNF-α, IL-6, and IL-10, enzyme-linked immunosorbent assay (ELISA) MAX Deluxe kits (BioLegend) were used according to the manufacturer's protocol. LCMV-specific antibody was detected by indirect ELISA. Briefly, microwell plates were coated with heat-inactivated LCMV in coating buffer (0.05 M carbonate/bicarbonate in distilled water, pH 9.6) at 4°C overnight. After blocking the plates with 1% bovine serum albumin (BSA), sera were dispensed into wells. After 2 h, goat anti-mouse IgG antibody conjugated with horseradish peroxidase (Enzo Clinical Labs, Farmingdale, NY, USA) was added. TMB substrate solution (SeraCare Life Sciences, Milford, MA, USA) was used for the colorimetric reaction. The optical density of each sample was measured using a Multiscan SkyHigh Microplate Spectrophotometer (Thermo Fisher Scientific).

Cytokine concentrations in serum were measured by the bead-based multiplex LEGENDplex analysis (LEGENDplex Mouse Inflammation Panel; BioLegend). Data that were collected on the Attune NxT Acoustic Focusing Cytometer (Thermo Fisher Scientific) were analyzed using LegendPLEX V8.0 software (BioLegend).

2.6 Intracellular staining for cytokines

Mouse splenocytes were incubated for 8 h in RPMI-1640 containing 1 μg/mL LCMV peptide glycoprotein$_{33–41}$ (GP33) or glycoprotein$_{61–80}$ (GP61) (GenScript, Piscataway, NJ, USA) and 2.5 μg/mL brefeldin A (Sigma-Aldrich). After surface staining with anti-mouse CD3-PerCP/Cy5.5, CD4-FITC, and CD8-FITC antibodies, the cells were fixed and permeabilized using the Foxp3/Transcription Factor Staining Buffer Kit (BioLegend) according to the manufacturer's protocol. Intracellular cytokines were detected using anti-mouse TNF-α-PE (Thermo Fisher Scientific) and IFN-γ-APC (BioLegend).

2.7 Real-time polymerase chain reaction

To measure the expression level of viral RNAs and cytokine mRNAs, total RNA was extracted using RNAiso Plus reagent (Takara Bio, Forster, CA, USA) or NucleoZOL (Macherey-Nagel, Düren, Germany), followed by cDNA synthesis by the ReverTraAce qPCR RT Kit (Toyobo, San Jose, CA, USA). Real-time quantitative polymerase chain reaction was performed using a CFX Connect Real-Time PCR System (Bio-Rad Laboratories, Hercules, CA, USA). The following primers were used: *GAPDH* forward 5′-TCAAGCTCATTTCCTGGTATGACA-3′, reverse 5′-TAGG GCCTCTCTTGCTCAGT-3′; *NP* forward 5′-CAGAAATGTTGAT

GCTGGACTGC-3′, reverse 5′-CAGACCTTGGCTTGCTTTACA CAG-3′; GP forward 5′-CATTCACCTGGACTTTGTCAGACTC-3′, reverse 5′-GCAACTGCTGTGTTCCCGAAAC-3′; *IFN-α* forward 5′-GGACTTTGGATTCCCGCAGGAGAAG-3′, reverse 5′-GCTGCAT CAGACAGCCTTGCAGGTC; *IFN-β* forward 5′-AACCTCACCTACA GGGCGGACTTCA-3′, reverse 5′-TCCCACGTCAATCTTTCCTCTTG CTTT-3′; IL-10 forward 5′-ATTTGAATTCCCTGGGTGAGAAG-3′, reverse 5′-CACAGGGGAGAAATCGATGACA-3′.

2.8 Flow cytometry

Cells were harvested and resuspended in flow cytometry buffer (PBS containing 1% BSA, 2 mM EDTA, and 0.1% sodium azide) and stained with the following antibodies purchased from BioLegend and Tonbo Biosciences (San Diego, CA, USA): GL7-FITC, B220-PerCP/Cy5.5, CD95-PE/Cy7, CD138-APC, PD-1-PE or PE/Cy7, CXCR5-APC/Cy7, F4/80-APC, CD86-FITC, CD40-PE, CD3-PerCP/Cy5.5 or APC/Cy7, CD4-FITC or APC/Cy7, and CD8-FITC or PerCP/Cy5.5. Data were acquired using the Attune NxT Acoustic Focusing Cytometer (Thermo Fisher Scientific) and analyzed with FlowJo software (BD Biosciences, San Diego, CA, USA).

2.9 RNA sequencing and data analysis

Total RNA from macrophages (M1 control group with M1 treatment group and M2 control group with M2 treatment group; 3 biological replicates per group) were isolated. An RNA sequencing (RNA-seq) library was then generated using the TruSeq Stranded mRNA Prep Kit with 101-bp paired-end reads. High-throughput sequencing was carried out using an Illumina (San Diego, CA, USA) NovaSeq 6000. FastQC (ver. 0.11.9, https://www.bioinformatics.babraham.ac.uk/projects/fastqc/) was utilized to assess the quality of raw paired-end reads. Raw mRNA-seq reads were filtered using Trim Galore! (ver. 0.6.3, https://github.com/FelixKrueger/TrimGalore) for adapter trimming. Consecutively, any bases with a Phred score—a measure of the quality of the identification of the nucleotide bases from automated sequencing—lower than Q30 or with read lengths lower than 80 bp were removed. Gene expression was accessed by mapping filtered reads to the *Mus musculus* reference genome (GRCm38.p6) with STAR (ver. 2.7.1a) using default parameters.[35] Acquired Sequence Alignment Map (SAM) files were converted to the binary version of SAM (BAM) files and then sorted using SAMtools (ver. 1.10-37-g2e4d43a)[36] using its implemented view and sort function. Differentially expressed genes (DEGs) were determined based on counts from the alignments using the Cufflinks package (ver. 2.2.1) with its implemented Cuffdiff extension.[37] The resulting output consisted of expression levels quantified as fragments per kilobase of exon per million, $\log_2$ fold change, and the *P* value of each transcript. A total of 52,149 genes were calculated for the analysis, of which 714 and 6,254 were determined to be significantly differentially expressed ($P < 0.05$) for M1 and M2 comparisons, respectively. Lists of significant DEGs were used for gene ontology (GO) term and Kyoto Encyclopedia of Genes and Genome (KEGG) pathway enrichment analysis using clusterProfiler, where genes were categorized to overrepresented GO terms or ranked KEGG pathways, followed by gene set enrichment analysis (GSEA).[38,39] The heatmap and volcano plot of the genes of interest were then displayed using the pheatmaps[40] and EnhancedVolcano[41] R packages, respectively. RNA-seq data used in this study have been deposited in the SRA database (NCBI) under accession code PRJNA809424.

2.10 Statistics

All parametric data were analyzed using unpaired Student *t* test or 1-way ANOVA with Bonferroni's post hoc test, and error bars indicate the standard error of the mean. GraphPad Prism (v.7) software (GraphPad Software, San Diego, CA, USA) was used for data analysis.

3 Results

3.1 Gal-4 differently regulates gene expression patterns in M1 and M2 macrophages

To investigate the effect of Gal-4 on gene expression profiles of M1 and M2 macrophages, we first performed transcriptome profiling on M1 and M2 macrophages in the presence or absence of Gal-4 by RNA-seq analysis. In this study, for convenience, we designated LPS-polarized macrophages as M1 and IL-4–polarized macrophages as M2.

A total of 714 DEGs (335 upregulated and 379 downregulated) were identified in M1 macrophages in response to Gal-4 treatment ($P < 0.05$) (Fig. 1A and Supplementary Table 1). In comparison, in M2 macrophages, a much greater number of DEGs (6,254, comprising 3,009 upregulated and 3,245 downregulated) were identified ($P < 0.05$) in response to Gal-4 treatment (Fig. 1B and Supplementary Table 1). Of note, besides the increased number of DEGs, we also observed more dramatic increases in fold changes in M2 macrophages compared to M1 macrophages upon Gal-4 treatment, as shown in the volcano plots (Fig. 1A and B) and cluster heatmap (Supplementary Fig. 2A and B) analyses. Moreover, as shown in the Venn diagram analysis, 133 (39.7% of DEGs in M1; 4.4% of DEGs in M2) and 166 (43.8% of DEGs in M1; 5.1% of DEGs in M2) genes were commonly upregulated and downregulated, respectively (Supplementary Fig. 2C and D). Interestingly, the multidimensional scaling plot shows that the changes induced by Gal-4 in M2 macrophages are distinct from those in M1 macrophages (Fig. 1C). These results indicate that Gal-4 may function differently in the gene expression regulation of M1 and M2 macrophages.

On the basis of these results, we next asked if Gal-4 treatment-induced DEGs are required for specific activation of certain types of macrophages. To answer this question, we further performed an overrepresentation analysis of the GO and KEGG pathway analysis. Our results showed that among upregulated DEGs in M1 macrophages in response to Gal-4, a total of 157 GO terms were enriched, whereas 2,490 were enriched in M2 macrophages (Supplementary Fig. 2E and Supplementary Table 2). Of note, consistent with the number of DEGs, the degree of enrichment was higher in M2 macrophages than in M1 macrophages, indicative of subtype specificity for Gal-4 treatment (Supplementary Fig. 2F). A similar effect was observed in enriched GO terms of downregulated DEGs (Supplementary Fig. 2G and H). Next, to rule out Gal-4–mediated common effects and specify the impact of Gal-4 on M1 and M2 macrophages, we performed KEGG pathway analysis and GSEA. Upon Gal-4 treatment, only 7 KEGG pathways (2 activated and 5 suppressed) were enriched in M1 macrophages (Fig. 1D and Supplementary Table 3), whereas 77 KEGG pathways (70 activated and 7 suppressed) were enriched in M2 macrophages (Fig. 1E and Supplementary Table 3), again suggesting a subtype specificity of Gal-4. Interestingly, activated pathways in M2 macrophages included antiviral immune response–associated pathways, such as "influenza A," "cytokine–cytokine receptor interaction," "coronavirus disease–COVID-19," "TNF signaling pathway," and "JAK-STAT signaling

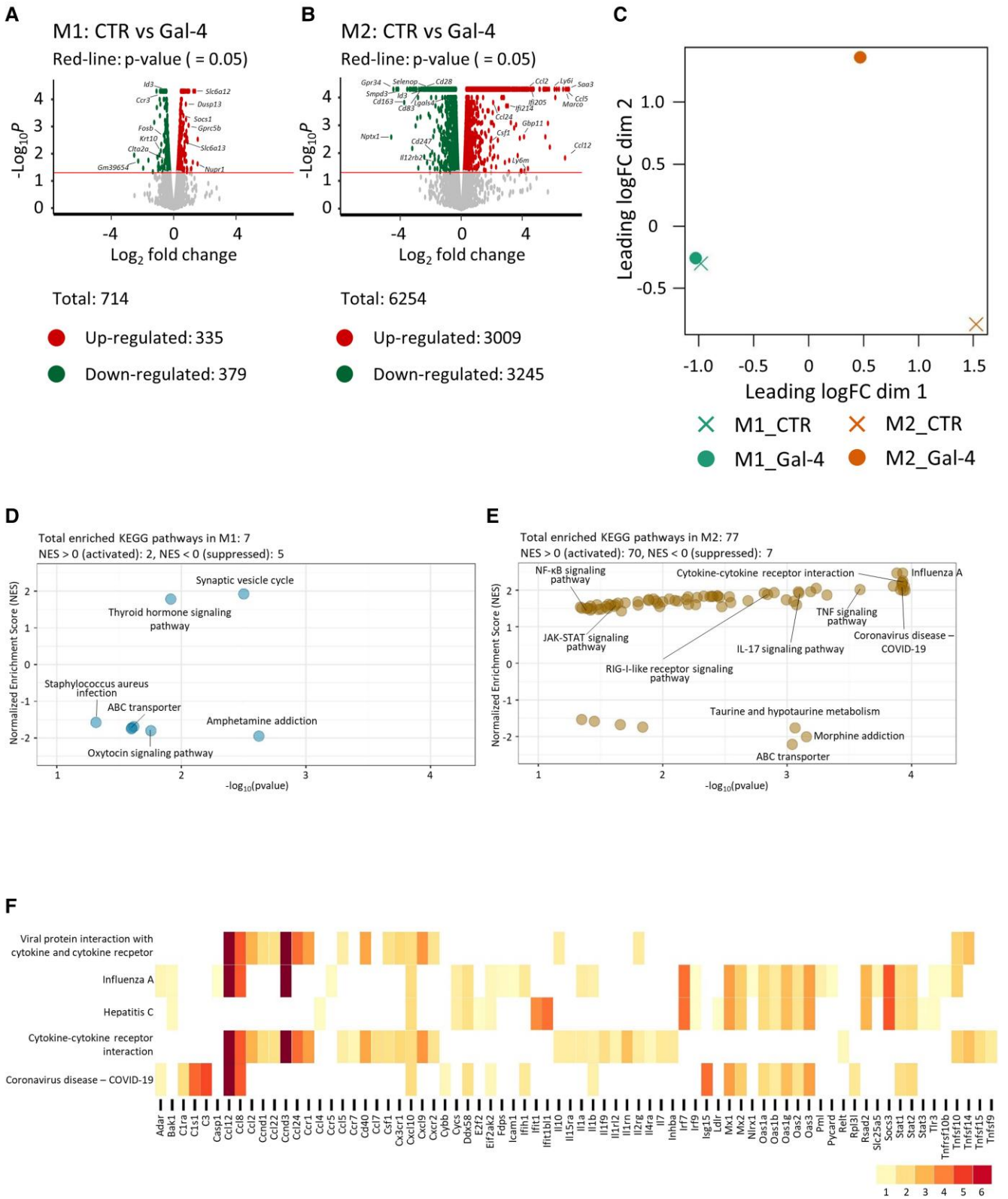

Fig. 1. Visualization of DEGs analyzed by RNA-seq. M1 or M2 macrophages were treated with Gal-4 (10 μg/mL) for 24 h at 37°C, 5% CO_2. Total RNA was extracted from the cells. RNA-seq data were derived from the mean value of 3 biological replicates. (A, B) Volcano plots showing DEGs of Gal-4–treated M1 (A) or M2 (B) macrophages. The solid line indicates *P* value cutoff, and the circles denote up- or downregulated genes. (C) Multidimensional scaling plot for RNA-seq data based on genes with fragments per kilobase of exon per million values higher than 0.2. (D, E) KEGG pathway GSEA was conducted ($P < 0.05$, $Q < 0.05$), and the results are represented as a plot. The x-axis is $-\log_{10}P$ of enriched pathways, and the y-axis is the normalized enrichment score (NES). Pathways are considered as activated or suppressed based on NES (activated: NES > 0, suppressed: NES < 0). (F) Heat plot reflecting fold change based on the 5 enriched KEGG pathways with the highest NES from M2 macrophages.

pathway." Furthermore, we focused on gene expression profiles in 5 pathways with the highest normalized enrichment score (NES), which revealed that Gal-4 could modulate M2 macrophages by activating pathways, including the viral immune response (Fig. 1F). Together, the RNA-seq analysis results reveal that Gal-4 may function specifically on M2 macrophages via induction of a unique transcriptome pattern that boosts immunostimulatory function.

3.2 Gal-4 enhances the activation of M2 macrophages upon Toll-like receptor 7 stimulation

To understand the molecular basis for the effect of Gal-4 on M1 and M2 macrophages, we sought to comprehensively interrogate Gal-4–specific downstream targets in the context of the characteristics of M2 macrophages. Unlike in M1 macrophages, Gal-4 robustly changed the gene expressions related to the antiviral immune response in M2 macrophages. These findings led us to focus on the effect of Gal-4 on the antiviral immune responses of M2 macrophages. To mimic the Toll-like receptor (TLR) stimulation by the virus, M2 macrophages were treated with Gal-4 in the presence or absence of R848, an agonist of TLR7 associated with viral RNA detection. As shown in Fig. 2, upon Gal-4 treatment, MHC-II, CD86, and CD40 were significantly upregulated, but MHC-I expression was not increased in M2 macrophages (Fig. 2A–D). Moreover, the expression of TNF-α, IL-6, IFN-α, and IL-10 in TLR7-stimulated M2 macrophages was significantly increased by Gal-4 treatment (Fig. 2E–H). Importantly, while Gal-4 or R848 alone exhibits marginal effects on the increase in IFN-α and IL-10 expressions, combinatorial treatment with Gal-4 and R848 significantly increased the expression of these cytokines (Fig. 2G and H). This result clearly shows that Gal-4 could enhance the M2 macrophage activation upon TLR7 stimulation. Also, considering the critical role of IFN-α and IL-10 in the generation and maintenance of antiviral adaptive responses including CD4/CD8 T-cell responses and antibody production,[42–44] synergistic stimulatory effects of Gal-4 and TLR7 stimulation on the expression of these cytokines in M2 macrophages could contribute to the enhanced antiviral immune responses. This increased immune response was dependent on the interaction between Gal-4 and glycans on M2 macrophages because treatment with β-lactose, a pan-galectin inhibitor, significantly blocked Gal-4–mediated increases in MHC-II, CD86, and CD40 expression on M2 macrophages in a dose-dependent manner (Supplementary Fig. 3A–C). Furthermore, when M2 macrophages were treated with Gal-4 in the presence of anti–Gal-4 antibody, increases in MHC-II, CD86, and CD40 expression mediated by Gal-4 treatment were significantly suppressed (Supplementary Fig. 3D–F). Based on our previous work[32] that Gal-4 binds to CD14 on human monocytes, Gal-4 might also bind to CD14 on M2 macrophages. To test this, we assessed whether an anti-CD14 neutralizing antibody could inhibit the immunostimulatory effects of Gal-4 on M2 macrophages. Anti-CD14 neutralizing antibody treatment significantly reduced the expression of CD86 and the production of IL-6 by Gal-4–treated M2 macrophages (Supplementary Fig. 3G and H). However, anti-CD14 neutralizing antibody did not completely abolish the effect of Gal-4. Thus, we could conclude that the interaction between Gal-4 and CD14 on M2 macrophages partially mediates the immunostimulatory effect of Gal-4.

Interestingly, Gal-4 alone also significantly increased the expressions of MHC-I, MHC-II, CD86, CD40, TNF-α, and IL-6 in M2 macrophages, even in the absence of TLR7 stimulation, which is consistent with our RNA-seq results (Fig. 2A–F). These results indicate that Gal-4 also exerts its function in the absence of TLR7 stimulation. By contrast, Gal-4 treatment did not significantly enhance the expressions of MHC-I, MHC-II, CD86, or CD40 on M1 macrophages regardless of R848 treatment (Supplementary Fig. 4A–D). In addition, the effect of Gal-4 on the expressions of activation markers and cytokines in unpolarized (M0) macrophages was assessed. Importantly, the immunoregulatory effect of Gal-4 on M0 macrophages was notably distinct from those on M1 and M2 macrophages. While Gal-4 hardly affected the expression of MHC-I, MHC-II, CD86, and CD40 on M1 macrophages (Supplementary Fig. 4), Gal-4 robustly changed the expression levels of these molecules on M0 (Supplementary Fig. 5) and M2 macrophages. Interestingly, the effect of Gal-4 on MHC-I and MHC-II was noticeably different between M0 and M2 macrophages. In M0 macrophages, Gal-4 significantly increased the expression of MHC-I but decreased the expression of MHC-II (Supplementary Fig. 5A and B). By contrast, in M2 macrophages, Gal-4 did not significantly change the expression of MHC-I, whereas MHC-II expression was significantly increased. These results support that Gal-4 differently regulates the activation of macrophages according to their differentiation states.

3.3 Gal-4 enhances immune response of LCMV-infected M2 macrophages

Given that TLR7 signaling has been identified to be critical for the development of an adaptive immune response sufficient to eliminate LCMV infection,[45] we expected Gal-4 to play a direct role in viral infection. Therefore, we examined whether Gal-4 could enhance the immune response of M2 macrophages upon viral infection. Expressions of MHC-II, CD86, and CD40, but not MHC-I, were significantly upregulated upon Gal-4 treatment in LCMV-infected M2 macrophages (Fig. 3A–D). Moreover, we observed increased production of proinflammatory cytokines TNF-α, IL-6, and IL-10 by LCMV-infected M2 macrophages in response to Gal-4 treatment (Fig. 3E–G). These results are consistent with our previous observation that Gal-4 enhanced the activation of TLR7-stimulated M2 macrophages (Fig. 2). We also found that Gal-4 treatment greatly increased the expression of type I IFNs, IFN-α, and IFN-β, which are critical players in the activation process of immune responses, as well as the suppression of viral replication (Fig. 3H and I). Correspondingly, the mRNA levels of LCMV nucleoprotein (NP) and LCMV glycoprotein (GP) were significantly decreased in Gal-4–treated M2 macrophages (Fig. 3J and K). However, Gal-4 treatment did not significantly change the NP expression level (Fig. 3L and M), indicating that Gal-4 does not significantly change the permeability of M2 macrophages to LCMV infection. Taken together, these results again point to Gal-4 as a novel key modulator of M2 macrophages and further verify its antiviral potential.

3.4 Gal-4–treated M2 macrophages enhance antiviral $CD4^+$ but not $CD8^+$ T-cell responses

Based on the in vitro observations mentioned above, we sought to assess the impact of Gal-4 on elevating the antiviral immune response of M2 macrophages in vivo. To this end, LCMV-infected M2 macrophages, either with or without Gal-4 treatment, were transferred intravenously into mice, and we screened for antiviral immune responses. Knowing that $CD8^+$ T cells are critical for the eradication of LCMV,[46,47] antiviral $CD8^+$ T-cell responses were analyzed. First, we compared the potential of LCMV-infected M2 macrophages to induce the proliferation of LCMV-specific $CD8^+$ T cells. No significant changes in the frequency of LCMV epitope

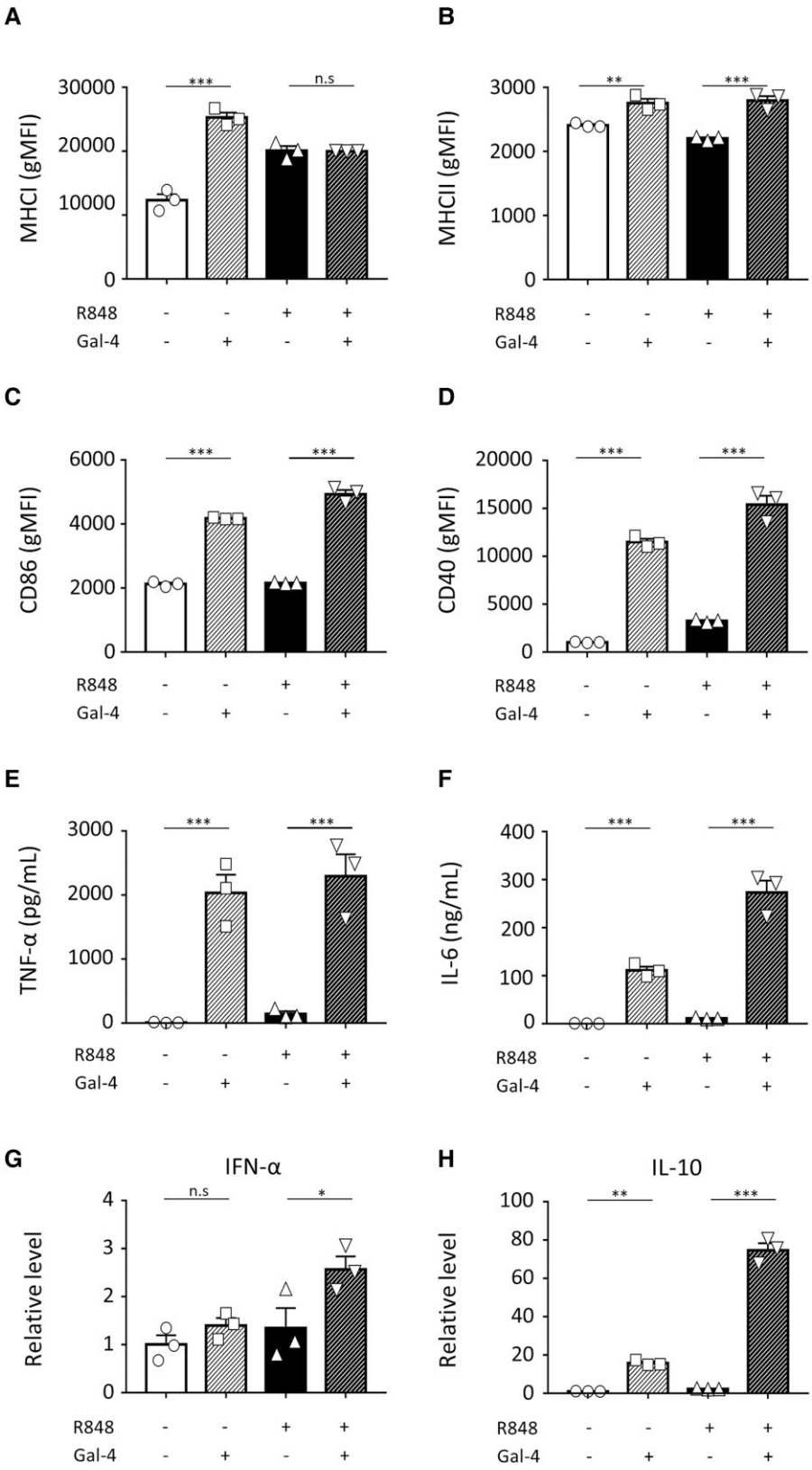

Fig. 2. Phenotypic and functional analysis of Gal-4–treated M2 macrophages with TLR7 stimulation. For TLR7 stimulation, M2 macrophages (2×10^5) were treated or untreated with R848 (1 μg/mL) for 24 h at 37°C, 5% CO_2. Simultaneously, a 10-μg/mL solution of Gal-4 was added. (A–D) The expression levels of (A) MHC-I, (B) MHC-II, (C) CD86, and (D) CD40 were measured by flow cytometry. (E, F) Productions of inflammatory cytokines (E) TNF-α and (F) IL-6 were detected by ELISA. (G, H) The expression levels of (G) IFN-α and (H) IL-10 were detected by real-time quantitative polymerase chain reaction 3 h after stimulation by Gal-4 (5 μg/mL). Each value is the mean ± SEM of 3 technical replicates. Asterisks indicate significant differences by 1-way ANOVA, followed by Bonferroni's post hoc test (*$P < 0.05$, **$P < 0.01$, ***$P < 0.001$). Experiments were conducted at least twice. gMFI, geometric mean fluorescence intensity.

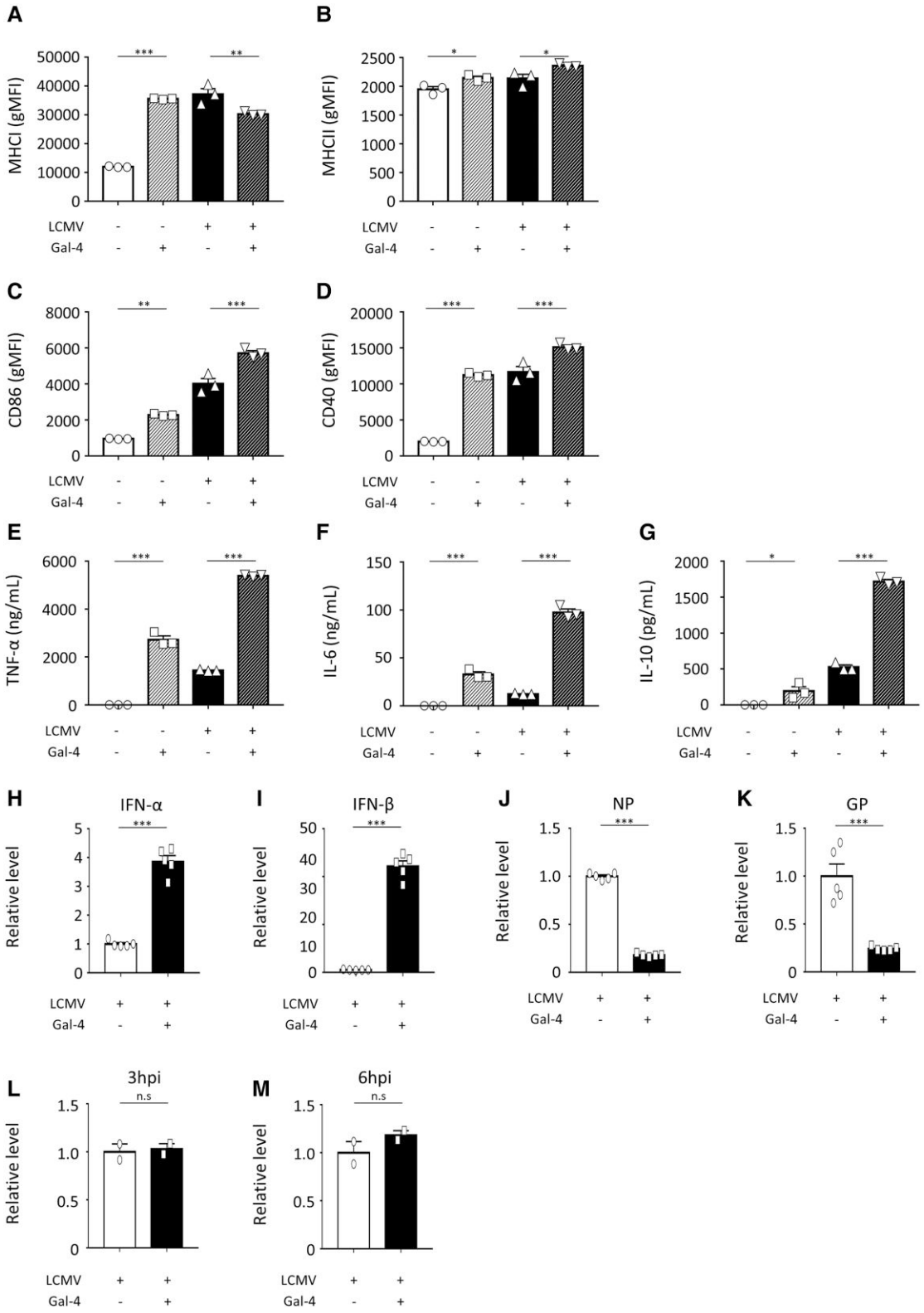

Fig. 3. Antiviral response of Gal-4–treated M2 macrophages. M2 macrophages (2×10^5) were infected with LCMV at 10 (A–D) or 3 (E–L) multiplicity of infection (MOI) in the presence or absence of Gal-4 (10 μg/mL). The cells were incubated at 37°C, 5% CO_2, and harvested at indicated times. (A–D) Bars indicate the expression levels of activation markers (A) MHC-I, (B) MHC-II, (C) CD86, and (D) CD40 24 h after infection. (E–G). After a 24-h incubation, the culture supernatant was harvested and assayed for (E) TNF-α, (F) IL-6, and (G) IL-10 by ELISA. (H, I) Real-time quantitative polymerase chain reaction (RT-qPCR) was performed to measure the expression levels of type I interferons (H) IFN-α and (I) IFN-β 6 h after infection. (J, K) At 24 h after infection, the RNA expression levels of (J) LCMV NP and (K) GP were detected by RT-qPCR with normalization to GAPDH. (L, M) Relative expression level of LCMV NP was detected at 3 h (L) and 6 h (M) postinfection. The mean ± SEM of technical replicates ($n \geq 2$) is shown. Asterisks indicate significant differences by unpaired *t* test or 1-way ANOVA, followed by Bonferroni's post hoc test (*$P < 0.05$, **$P < 0.01$, ***$P < 0.001$). All experiments were conducted at least twice. gMFI, geometric mean fluorescence intensity.

GP33-tetramer$^+$ and nucleoprotein$_{396–404}$ (NP396)–tetramer$^+$ CD8$^+$ T cells in blood, livers, and spleens were observed (Fig. 4A–F). Similarly, Gal-4–treated, LCMV-infected M2 macrophages did not significantly increase IFN-γ– and TNF-α–producing antiviral CD8$^+$ T cells in blood, livers, and spleens (Fig. 4G–I). These results demonstrate that Gal-4 may not enhance the ability of M2 macrophages to promote antiviral CD8$^+$ T-cell responses.

Given the above finding that Gal-4 treatment induced selective expression of MHC-II in contrast to MHC-I, we suspected that Gal-4 has a role in CD4$^+$ T-cell activation. Thus, we analyzed whether Gal-4 treatment of LCMV-infected M2 macrophages could enhance antiviral CD4$^+$ T-cell responses. In contrast to CD8$^+$ T-cell responses, Gal-4–treated, LCMV-infected M2 macrophages significantly increased the frequency of LCMV glycoprotein$_{66–77}$ (GP66)–tetramer$^+$ CD4$^+$ T cells in blood (Fig. 5A). Similarly, IFN-γ–producing CD4$^+$ T cells were significantly increased in blood with Gal-4–treated, LCMV-infected M2 macrophages (Fig. 5B). We obtained similar results in livers (Fig. 5C and D). Although a significant increase in LCMV GP66-tetramer$^+$ and IFN-γ–producing CD4$^+$ T cells was not observed in spleens (Fig. 5E and F), follicular helper T (T_{fh}) cells (CD4$^+$CXCR5$^+$PD-1$^+$) were significantly increased in spleens with Gal-4–treated, LCMV-infected M2 macrophages (Fig. 5G). T_{fh} cells localized within B-cell follicles of secondary lymphoid organs are crucial in promoting B-cell differentiation into antibody-producing plasma cells. This result led us to analyze the production of LCMV-specific antibodies in mice with LCMV-infected M2 macrophages with or without Gal-4 treatment. A significantly high amount of LCMV-specific antibodies was detected in mice serum with Gal-4–treated, LCMV-infected M2 macrophages (Fig. 5H). Together, these findings indicate that Gal-4 enhances the antiviral ability of M2 macrophages by activation of CD4$^+$ T-cell responses, subsequently enhancing antibody production.

3.5 Gal-4 administration augments antiviral immune responses in vivo

We finally sought to investigate whether the administration of Gal-4 boosts the antiviral immune response in vivo. To this end, LCMV-infected mice were injected intraperitoneally with Gal-4 (2.5 mg/kg) once per day for 5 d. In agreement with our results from the macrophage adoptive transfer experiment (Fig. 5), Gal-4 administration significantly increased the LCMV-specific antibody level in serum (Fig. 6B). To substantiate the relevance of augmented antibody response with Gal-4 administration, we further analyzed the proportion of splenic germinal center (GC) B cells (GL7$^+$, CD95$^+$), antibody-secreting B cells (CD138$^+$, B220^{low}), and T_{fh}, which are highly responsible for Ag-specific B-cell differentiation and antibody formation. The proportion of GC B cells (Fig. 6C), antibody-secreting cells (Fig. 6D), and T_{fh} (Fig. 6E) was significantly increased in the spleens of Gal-4–treated mice. Considering that the interaction between GC B cells and T_{fh} cells is crucial for the generation of humoral response, these results clearly demonstrated that Gal-4 enhances antiviral immune responses in vivo by increasing the antibody production and the frequency of B and T_{fh} cells in the spleen. In addition, we measured serum IFN-γ level that was known to play a major role in LCMV-induced inflammation, possibly leading to fatal diseases.[48,49] Interestingly, Gal-4 treatment significantly reduced serum IFN-γ level at 7 days post infection (dpi) as compared to untreated mice (Fig. 6F). This result suggests that Gal-4–mediated antiviral immunity could result in the relieved immunopathologic outcomes.

4 Discussion

Most proteins of mammalian cells have glycans, and the interactions of glycans with glycan-binding proteins, such as galectins, play critical roles in innate and adaptive immune responses.[17] The ability of galectins to bind glycan can be used for recognizing some pathogenic microorganisms and lead to the initiation of innate immunity.[22,50] Furthermore, galectins are known to promote antitumor immunity, angiogenesis,[18] and the progression of autoimmune diseases.[19] Despite many efforts to decipher the pathophysiologic roles of the galectin family,[51] the immunologic relevance of Gal-4 has remained enigmatic. In this study, we demonstrate that Gal-4 distinctively regulates the function of M1 and M2 macrophages. While Gal-4 induced dramatic changes in the gene expression patterns of M2 macrophages, it induced relatively fewer substantial changes in M1 macrophages. Interestingly, Gal-4 activated the antiviral response–related genes in M2 macrophages. Consistent with these results, the concomitant treatment of M2 macrophages with TLR7 agonist and Gal-4 increased MHC-II, CD86, and CD40 expressions and enhanced the production of inflammatory cytokines, such as TNF-α and IL-6. There are several hypotheses to explain the different effects of Gal-4 on M1 and M2 macrophages. First, M2 macrophages might express more Gal-4 receptors compared to M1 macrophages. Second, glycosylation patterns of Gal-4 receptors might differ between M1 and M2 macrophages. Last, different intracellular components between the 2 macrophage subsets that are associated with the Gal-4 signaling pathway could elicit different effects. Due to the current knowledge gap about the identity of the receptor on macrophages that cross-link with Gal-4, further investigation is needed to identify Gal-4–binding receptors on M1 and M2 macrophages and their glycosylation status.

We observed that Gal-4 alone, without TLR stimulation, also had immunostimulatory effects on M2 macrophages. Therefore, Gal-4 could activate M2 macrophages not only in viral infection conditions where TLR signaling was activated but also in noninfection conditions, such as the M2 abundant tumor microenvironment. Considering our result that the immunostimulatory activity of Gal-4 was augmented rather than inhibited in the presence of TLR7 stimulation (Fig. 2) or LCMV infection (Fig. 3), Gal-4 could be applied to the treatment of diseases associated with M2 macrophages, such as chronic viral infections as well as cancers.

Our results indicate that Gal-4 could ultimately enhance the antiviral response of CD4$^+$ T cells through M2 macrophage activation by increasing the number and functionality of CD4$^+$ T cells, leading to an increase in antibody production against LCMV. However, in contrast to CD4$^+$ T cells, the number and functionality of antiviral CD8$^+$ T cells were not significantly changed by Gal-4–treated M2 macrophages. Interestingly, while the expression of MHC-II on M2 macrophages was significantly increased by Gal-4 treatment, the expression of MHC-I was not (Fig. 2). We believe this phenomenon accounts for how Gal-4 differently regulates antiviral CD8$^+$ and CD4$^+$ T-cell responses induced by M2 macrophages.

Considering the dynamic functionality and plasticity of macrophages, maintaining the balance of the M1/M2 paradigm is crucial to immune homeostasis. Liu et al.[52] revealed that polarized macrophages have the potential to repolarize into another state with a corresponding cytokine milieu. Interestingly, our results suggest that Gal-4 could enhance the immunostimulatory properties of

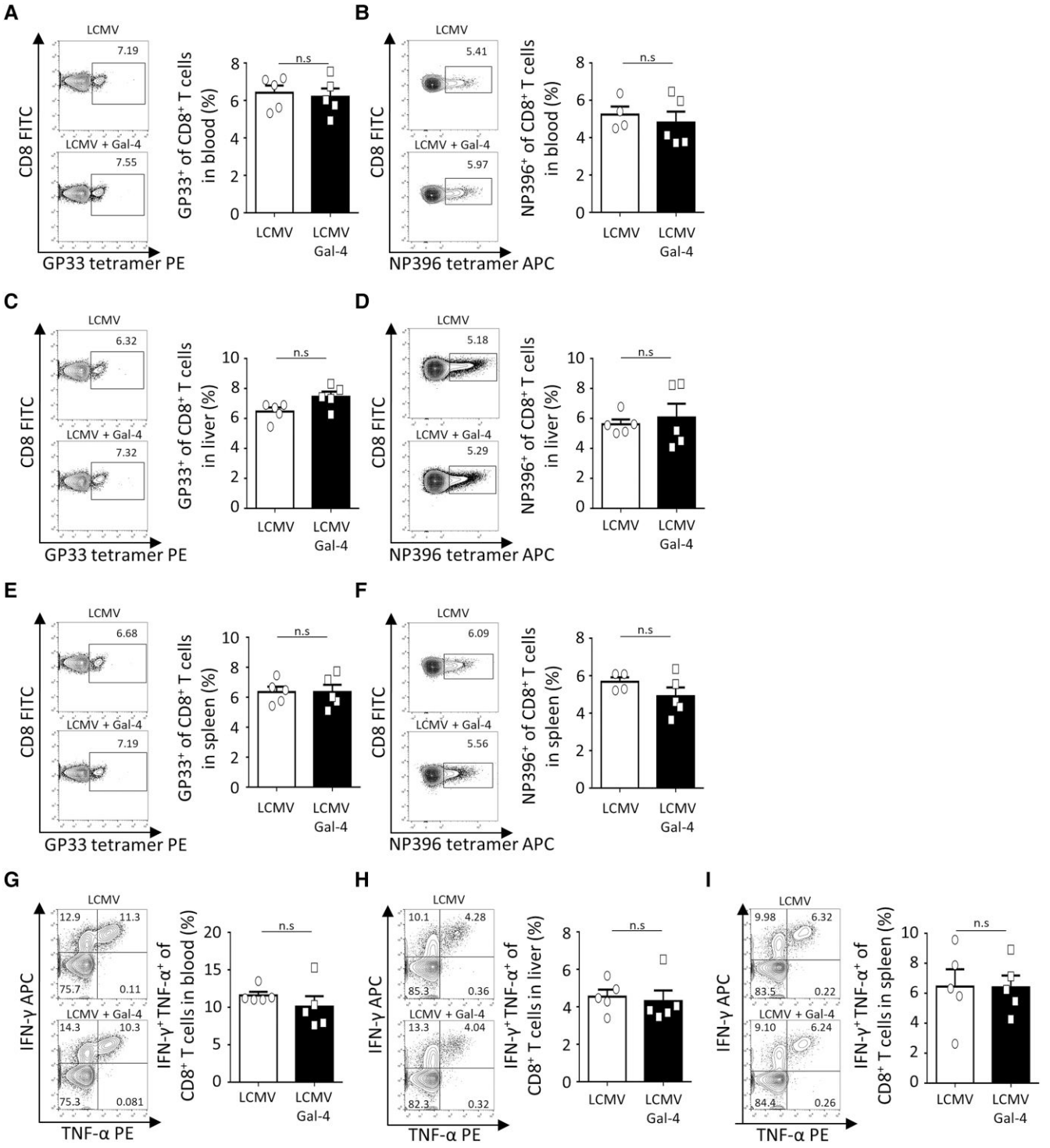

Fig. 4. Antiviral response of CD8+ T cells after adoptive transfer of LCMV-infected M2 macrophages treated with Gal-4. Phenotype and functionality of LCMV-specific CD8+ were analyzed by flow cytometry and compared between Gal-4–untreated and Gal-4–treated LCMV-infected M2 macrophage recipients. (A–F) Percentage of GP33-tetramer+ or NP396-tetramer+ CD8+ T cells and representative flow cytometry plots in (A, B) blood, (C, D) liver, and (E, F) spleen are shown. (G–I) After stimulation of splenocytes with GP33 peptides, the proportions of TNF-α– and IFN-γ–secreting CD8+ T cells in (G) blood, (H) liver, and (I) spleen are shown with representative flow cytometry plots. Refer to Supplementary Fig. 6A for the gating strategy. Experiments were conducted at least twice, and each value is the mean ± SEM of technical replicates ($n \geq 4$).

M2 macrophages. Macrophages are critical elements of the immune system and have a role in defense against viruses. However, some viruses, such as hepatitis C, foot-and-mouth disease virus, measles virus, and human immunodeficiency virus 1, are known to adopt a strategy to differentiate into M2-like macrophages to evade, prevent, or delay host immune mechanisms.[14] Despite the important role that M2 macrophages exhibit during chronic infection, therapeutic approaches targeting M2

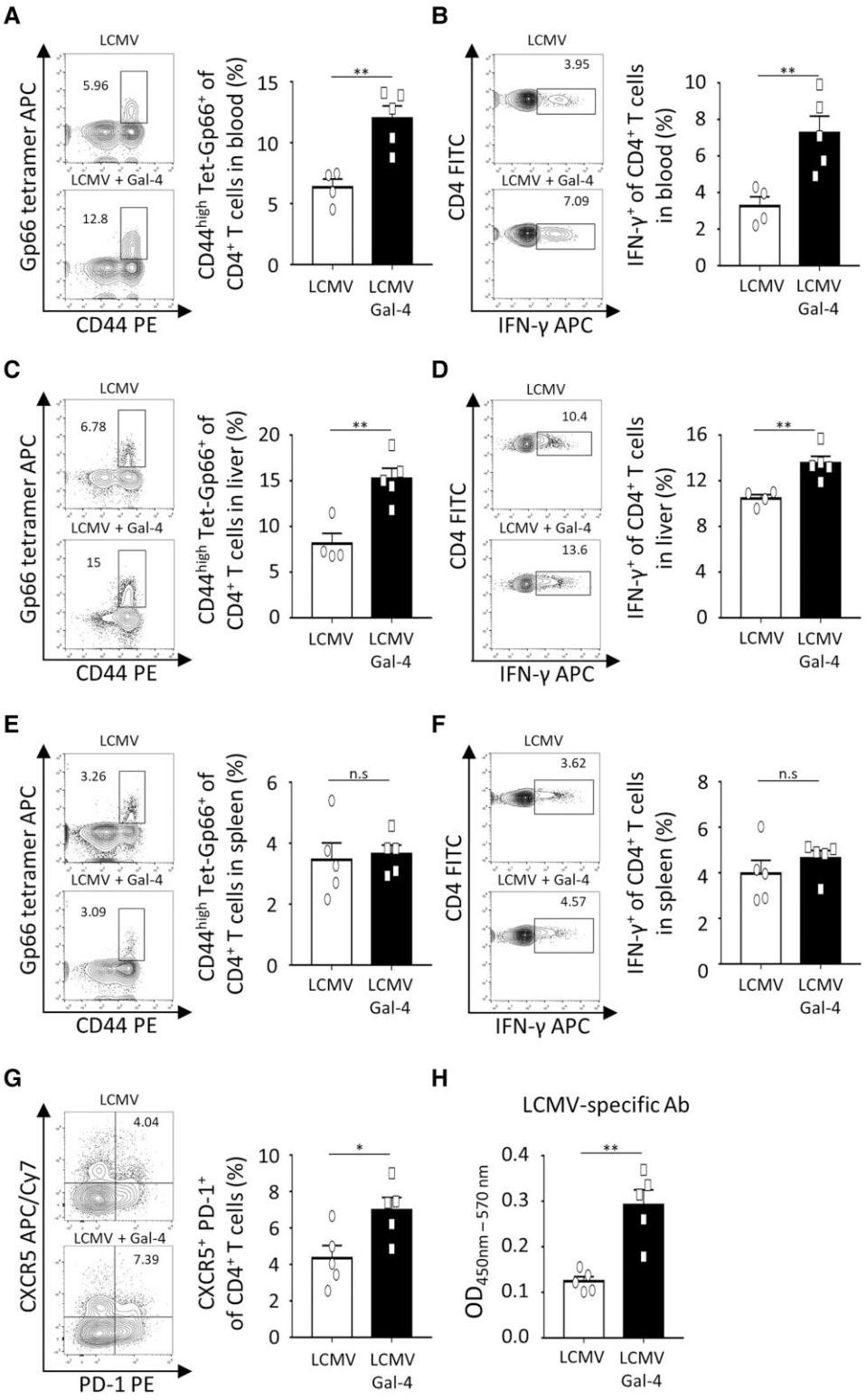

Fig. 5. CD4+ T-cell response against LCMV after adoptive transfer of Gal-4–treated, LCMV-infected M2 macrophages. CD4+ T cells and serum were collected from the recipient mice, which received Gal-4–untreated or Gal-4–treated LCMV-infected M2 macrophages to analyze the antiviral response. Splenocytes were stimulated with LCMV GP61 peptide to analyze the proportion of IFN-γ–secreting CD4+ T cells using flow cytometry. (A–F) Representative flow cytometry plots and the percentage of GP66-tetramer+– or IFN-γ–secreting CD4+ T cells in (A, B) blood, (C, D) liver, and (E, F) spleen. (G) CXCR5+ PD-1+ cells among CD4+ T cells are shown, with the representative flow cytometry plot and the graph showing the percentages. (H) The optical density of LCMV-specific antibodies from serum was measured by indirect ELISA. Refer to Supplementary Fig. 6B for the gating strategy. All experiments were performed at least twice, and each value represents the mean ± SEM of technical replicates ($n \geq 4$). Asterisks indicate significant differences by unpaired *t* test (*$P < 0.05$, **$P < 0.01$).

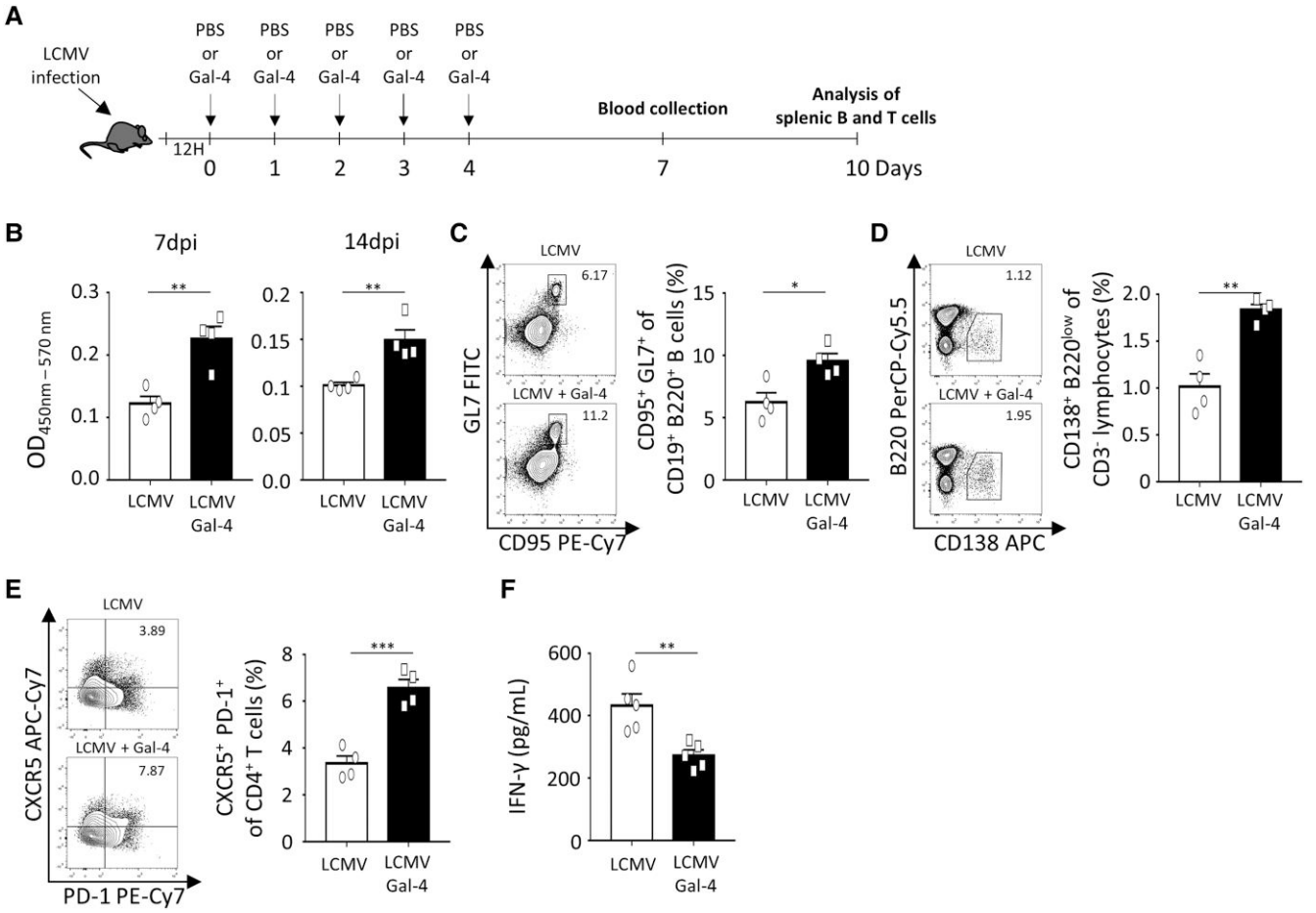

Fig. 6. Antiviral effect of Gal-4 administration in LCMV-infected mice. Mice were infected with 1×10^5 focus forming units (FFU) of LCMV Armstrong strain and administrated with Gal-4 (2.5 mg/kg) intraperitoneally once per day for 5 d. Spleen and blood were collected from mice at indicated time points to analyze the antiviral immune response. (A) Schematic experimental layout to analyze antiviral immune response. (B) LCMV-specific antibodies from serum were measured by indirect ELISA at 7 or 14 days post infection (dpi). (C, D) The representative flow cytometry plot and the percentage of $CD95^+$ $GL7^+$ germinal center B cells (C) and $CD138^+$ $B220^{low}$ antibody-secreting B cells (D) in spleen at 10 dpi are shown. (E) The proportion of PD-1^+ $CXCR5^+$ T_{fh} cells was measured by flow cytometry with representative plots and graphs. Refer to Supplementary Fig. 6B and C for the gating strategy. (F) The level of IFN-γ in serum at 7 dpi was measured by LEGNEDplex analysis. Values are the mean ± SEM of 4 to 5 mice, and all experiments were performed at least twice. Asterisks indicate significant differences by unpaired *t* test (*$P < 0.05$, **$P < 0.01$, ***$P < 0.001$).

macrophages are not well understood. The novel immunomodulatory function of Gal-4 to promote the clearance of virus within M2 macrophages (Fig. 3) but also the antibody production mediated by $CD4^+$ T cells (Fig. 5) indicates potential therapeutic agents, such as antiviral drugs, against chronic viruses and adjuvants of virus vaccine.

This is noteworthy because an increased immune response of M2 macrophages has been reported to accompany several clinical benefits. Tumor-associated macrophages (TAMs) resemble the features of M2 macrophages in the context of suppressed immune response and are known to promote the growth of tumor cells. Thus, repolarization of TAMs to an immune-activating form has been highlighted for cancer therapy.[15,53,54] Targeting molecular pathways, such as the NF-κB and STAT pathways, essential for the M1 tumoricidal functions, holds great promise for anticancer therapy.[53,54] Here, we demonstrate that Gal-4 significantly induced the activation of those pathways (Fig. 1E) and associated functions, such as the inflammatory cytokine production and the expression of type I IFN-associated genes (Fig. 1F and Fig. 2). Although the activation of those pathways is not always beneficial for anticancer therapy, the immunomodulatory function of Gal-4 on M2 macrophages sheds light on the novel anticancer potential of Gal-4.

Taken together, the enhanced antiviral response of M2 macrophages by Gal-4 and subsequent activation of $CD4^+$ T cells by M2 macrophages upon Gal-4 treatment indicate that Gal-4 has an immunomodulatory function on M2 macrophages. Our findings provide insight for developing a therapy for cancer and chronic viral infection utilizing this biased differentiation toward M2 macrophages in the M1/M2 paradigm.

Authorship

Y.S., S.H., and J.K. provided conceptualization and design of study. I.L., Y.J., H.J., R.J., E.K., and S.E. performed experiments. I.L., Y.J., H.J., J.K., R.J., E.K., H.C., S.E., Y.S., and S.H. interpreted data. I.L., J.K., R.J., and H.C. wrote the original draft. S.E., Y.S., S.H., and J.K. reviewed and edited the manuscript. All authors read and approved the final version of the manuscript.

Acknowledgments

This research was supported by the National Research Foundation of Korea (NRF) grant funded by the Korean government (No. 2021R1I1A1A01041639 and NRF-2021R1C1C1012962)

and the Chung-Ang University Graduate Research Scholarship in 2020. We acknowledge the NIH Tetramer Core Facility for providing LCMV GP33, NP396, and GP66 tetramers.

Supplementary material

Supplementary material is available at *Journal of Leukocyte Biology Journal* online.

Disclosures

The authors declare no financial/commercial conflicts of interest.

Data availability

The data that support the findings of this study are available from the corresponding authors upon reasonable request.

Ethics approval for animal studies

Approval for the animal protocols was received from the Institutional Animal Care and Use Committee at Institut Pasteur Korea (approval number: IPK-21002).

References

1. Johnston RB Jr. Current concepts: immunology. Monocytes and macrophages. *N Engl J Med*. 1988:318(12):747–752.
2. Varol C, Mildner A, Jung S. Macrophages: development and tissue specialization. *Annu Rev Immunol*. 2015:33(1):643–675.
3. Locati M, Curtale G, Mantovani A. Diversity, mechanisms, and significance of macrophage plasticity. *Annu Rev Pathol*. 2020:15(1):123–147.
4. Yunna C, Mengru H, Lei W, Weidong C. Macrophage M1/M2 polarization. *Eur J Pharmacol*. 2020:877:173090.
5. Martinez FO, Gordon S. The M1 and M2 paradigm of macrophage activation: time for reassessment. *F1000Prime Rep*. 2014:6:13.
6. Stein M, Keshav S, Harris N, Gordon S. Interleukin 4 potently enhances murine macrophage mannose receptor activity: a marker of alternative immunologic macrophage activation. *J Exp Med*. 1992:176(1):287–292.
7. Murray PJ, Allen JE, Biswas SK, Fisher EA, Gilroy DW, Goerdt S, Gordon S, Hamilton JA, Ivashkiv LB, Lawrence T, *et al.* Macrophage activation and polarization: nomenclature and experimental guidelines. *Immunity*. 2014:41(1):14–20.
8. Benoit M, Desnues B, Mege JL. Macrophage polarization in bacterial infections. *J Immunol*. 2008:181(6):3733–3739.
9. O'Reilly M, Newcomb DE, Remick D. Endotoxin, sepsis, and the primrose path. *Shock*. 1999:12(6):411–420.
10. Funes SC, Rios M, Escobar-Vera J, Kalergis AM. Implications of macrophage polarization in autoimmunity. *Immunology*. 2018:154(2):186–195.
11. Shapouri-Moghaddam A, Mohammadian S, Vazini H, Taghadosi M, Esmaeili SA, Mardani F, *et al.* Macrophage plasticity, polarization, and function in health and disease. *J Cell Physiol*. 2018:233(9):6425–6440.
12. Martinez FO, Sica A, Mantovani A, Locati M. Macrophage activation and polarization. *Front Biosci*. 2008:13(2):453–461.
13. Wang LX, Zhang SX, Wu HJ, Rong XL, Guo J. M2b macrophage polarization and its roles in diseases. *J Leukoc Biol*. 2019:106(2):345–358.
14. Sang Y, Miller LC, Blecha F. Macrophage polarization in virus-host interactions. *J Clin Cell Immunol*. 2015:6(2):311.
15. Chanmee T, Ontong P, Konno K, Itano N. Tumor-associated macrophages as major players in the tumor microenvironment. *Cancers (Basel)*. 2014:6(3):1670–1690.
16. Liu FT. Regulatory roles of galectins in the immune response. *Int Arch Allergy Immunol*. 2005:136(4):385–400.
17. Thiemann S, Baum LG. Galectins and immune responses—just how do they do those things they do? *Annu Rev Immunol*. 2016:34:243–264.
18. Mendez-Huergo SP, Blidner AG, Rabinovich GA. Galectins: emerging regulatory checkpoints linking tumor immunity and angiogenesis. *Curr Opin Immunol*. 2017:45:8–15.
19. Toscano MA, Martinez Allo VC, Cutine AM, Rabinovich GA, Marino KV. Untangling galectin-driven regulatory circuits in autoimmune inflammation. *Trends Mol Med*. 2018:24(4):348–363.
20. Barondes SH, Cooper DN, Gitt MA, Leffler H. Galectins. Structure and function of a large family of animal lectins. *J Biol Chem*. 1994:269(33):20807–20810.
21. Rubinstein N, Ilarregui JM, Toscano MA, Rabinovich GA. The role of galectins in the initiation, amplification and resolution of the inflammatory response. *Tissue Antigens*. 2004:64(1):1–12.
22. Vasta GR. Roles of galectins in infection. *Nat Rev Microbiol*. 2009:7(6):424–438.
23. Leffler H, Carlsson S, Hedlund M, Qian Y, Poirier F. Introduction to galectins. *Glycoconj J*. 2002:19(7–9):433–440.
24. Nabi IR, Shankar J, Dennis JW. The galectin lattice at a glance. *J Cell Sci*. 2015:128(13):2213–2219.
25. Wasano K, Hirakawa Y. Two domains of rat galectin-4 bind to distinct structures of the intercellular borders of colorectal epithelia. *J Histochem Cytochem*. 1999:47(1):75–82.
26. Danielsen EM, van Deurs B. Galectin-4 and small intestinal brush border enzymes form clusters. *Mol Biol Cell*. 1997:8(11):2241–2251.
27. Oda Y, Herrmann J, Gitt MA, Turck CW, Burlingame AL, Barondes SH, Leffler H. Soluble lactose-binding lectin from rat intestine with two different carbohydrate-binding domains in the same peptide chain. *J Biol Chem*. 1993:268(8):5929–5939.
28. Markova V, Smetana K, Jr., Jenikova G, Lachova J, Krejcirikova V, Poplstein M, Fábry M, Brynda J, Alvarez RA, Cummings RD, *et al.* Role of the carbohydrate recognition domains of mouse galectin-4 in oligosaccharide binding and epitope recognition and expression of galectin-4 and galectin-6 in mouse cells and tissues. *Int J Mol Med*. 2006:18(1):65–76.
29. Hokama A, Mizoguchi E, Sugimoto K, Shimomura Y, Tanaka Y, Yoshida M, Rietdijk ST, de Jong YP, Snapper SB, Terhorst C, *et al.* Induced reactivity of intestinal CD4(+) T cells with an epithelial cell lectin, galectin-4, contributes to exacerbation of intestinal inflammation. *Immunity*. 2004:20(6):681–693.
30. Paclik D, Danese S, Berndt U, Wiedenmann B, Dignass A, Sturm A. Galectin-4 controls intestinal inflammation by selective regulation of peripheral and mucosal T cell apoptosis and cell cycle. *PLoS One*. 2008:3(7):e2629.
31. de Jong C, Stancic M, Pinxterhuis TH, van Horssen J, van Dam AM, Gabius HJ, Baron W. Galectin-4, a negative regulator of oligodendrocyte differentiation, is persistently present in axons and microglia/macrophages in multiple sclerosis lesions. *J Neuropathol Exp Neurol*. 2018:77(11):1024–1038.
32. Hong SH, Shin JS, Chung H, Park CG. Galectin-4 interaction with CD14 triggers the differentiation of monocytes into macrophage-like cells via the MAPK signaling pathway. *Immune Netw*. 2019:19(3):e17.
33. Weischenfeldt J, Porse B. Bone marrow-derived macrophages (BMM): isolation and applications. *CSH Protoc*. 2008:2008:pdb prot5080.

34. Battegay M, Cooper S, Althage A, Banziger J, Hengartner H, Zinkernagel RM. Quantification of lymphocytic choriomeningitis virus with an immunological focus assay in 24- or 96-well plates. *J Virol Methods*. 1991:33(1–2):191–198.
35. Dobin A, Davis CA, Schlesinger F, Drenkow J, Zaleski C, Jha S, Batut P, Chaisson M, Gingeras TR. STAR: ultrafast universal RNA-seq aligner. *Bioinformatics*. 2013:29(1):15–21.
36. Li H, Handsaker B, Wysoker A, Fennell T, Ruan J, Homer N, Marth G, Abecasis G, Durbin R. The sequence alignment/map FORMAT and SAMtools. *Bioinformatics*. 2009:25(16):2078–2079.
37. Trapnell C, Roberts A, Goff L, Pertea G, Kim D, Kelley DR, Pimentel H, Salzberg SL, Rinn JL, Pachter L. Differential gene and transcript expression analysis of RNA-seq experiments with TopHat and Cufflinks. *Nat Protoc*. 2012:7(3):562–578.
38. Yu G, Wang LG, Han Y, He QY. clusterProfiler: an R package for comparing biological themes among gene clusters. *OMICS*. 2012:16(5):284–287.
39. Subramanian A, Tamayo P, Mootha VK, Mukherjee S, Ebert BL, Gillette MA, Paulovich A, Pomeroy SL, Golub TR, Lander ES, *et al.* Gene set enrichment analysis: a knowledge-based approach for interpreting genome-wide expression profiles. *Proc Natl Acad Sci U S A*. 2005:102(43):15545–15550.
40. Kolde R. pheatmap: Pretty Heatmaps. 2019. R package version 1.0.12. https://CRAN.R-project.org/package=pheatmap.
41. Blighe K, Rana S, Lewis M. EnhancedVolcano: publication-ready volcano plots with enhanced colouring and labeling. 2022. R package version 1.14.0. https://github.com/kevinblighe/EnhancedVolcano.
42. Seo YJ, Hahm B. Type I interferon modulates the battle of host immune system against viruses. *Adv Appl Microbiol*. 2010:73:83–101.
43. Laidlaw BJ, Lu Y, Amezquita RA, Weinstein JS, Vander Heiden JA, Gupta NT, Kleinstein SH, Kaech SM, Craft J. Interleukin-10 from CD4(+) follicular regulatory T cells promotes the germinal center response. *Sci Immunol*. 2017:2(16):eaan4767.
44. Tian Y, Mollo SB, Harrington LE, Zajac AJ. IL-10 regulates memory T Cell development and the balance between Th1 and follicular Th cell responses during an acute viral infection. *J Immunol*. 2016:197(4):1308–1321.
45. Walsh KB, Teijaro JR, Zuniga EI, Welch MJ, Fremgen DM, Blackburn SD, von Tiehl KF, Wherry EJ, Flavell RA, Oldstone MBA. Toll-like receptor 7 is required for effective adaptive immune responses that prevent persistent virus infection. *Cell Host Microbe*. 2012:11(6):643–653.
46. Fung-Leung WP, Kundig TM, Zinkernagel RM, Mak TW. Immune response against lymphocytic choriomeningitis virus infection in mice without CD8 expression. *J Exp Med*. 1991:174(6):1425–1429.
47. Nansen A, Jensen T, Christensen JP, Andreasen SØ, Röpke C, Marker O, Thomsen AR. Compromised virus control and augmented perforin-mediated immunopathology in IFN-γ-deficient mice infected with lymphocytic choriomeningitis virus. *J Immunol* 1999:163(11):6114–6122.
48. Nansen A, Christensen JP, Ropke C, Marker O, Scheynius A, Thomsen AR. Role of interferon-gamma in the pathogenesis of LCMV-induced meningitis: unimpaired leucocyte recruitment, but deficient macrophage activation in interferon-gamma knock-out mice. *J Neuroimmunol*. 1998:86(2):202–212.
49. Leist TP, Eppler M, Zinkernagel RM. Enhanced virus replication and inhibition of lymphocytic choriomeningitis virus disease in anti-gamma interferon-treated mice. *J Virol*. 1989:63(6):2813–2819.
50. Lee JH, Park JH. Host-microbial interactions in metabolic diseases: from diet to immunity. *J Microbiol*. 2022:60(6):561–575.
51. Cao ZQ, Guo XL. The role of galectin-4 in physiology and diseases. *Protein Cell*. 2016:7(5):314–324.
52. Liu SX, Gustafson HH, Jackson DL, Pun SH, Trapnell C. Trajectory analysis quantifies transcriptional plasticity during macrophage polarization. *Sci Rep*. 2020:10(1):12273.
53. Tang X, Mo C, Wang Y, Wei D, Xiao H. Anti-tumour strategies aiming to target tumour-associated macrophages. *Immunology*. 2013:138(2):93–104.
54. Zheng X, Turkowski K, Mora J, Brune B, Seeger W, Weigert A, Savai R. Redirecting tumor-associated macrophages to become tumoricidal effectors as a novel strategy for cancer therapy. *Oncotarget*. 2017:8(29):48436–48452.